



Estimating the Hubble constant from the mock GW data of Einstein Telescope

Pinaki Roy

Supervisor: Prof. Tomasz Bulik

Astronomical Observatory of the University of Warsaw,
Al. Ujazdowskie 4, 00-478 Warsaw, Poland

1. Einstein Telescope
2. Gravitational Wave Astronomy
3. Cosmology
 - Λ CDM model
 - Hubble Tension
4. Method
 - Mock data
 - Analysis
5. Results
6. Conclusion

Einstein Telescope

- ★ ET is a proposed Gen III gravitational wave detector
- ★ Tenfold better sensitivity than present Gen II detectors
- ★ GW bandwidth: 1 Hz – 10 kHz (LIGO: 10 – 1000 Hz)
- ★ Located underground at a depth of 100–300 m to reduce noise

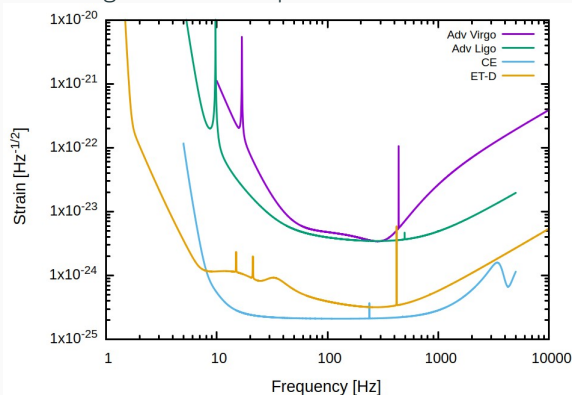


Figure 1: Amplitude spectral density of ET

- ★ Currently accepted ET design is called ET-D.
- ★ Equilateral triangle configuration with arm-length 10 km
- ★ 2-band xylophone design with 6 interferometers
- ★ Low Frequency (1 – 40 Hz); High Frequency (40 Hz – 10 kHz)
- ★ Sensitive to GW from all directions without any blind spot
- ★ Can generate null streams useful to eliminate glitches

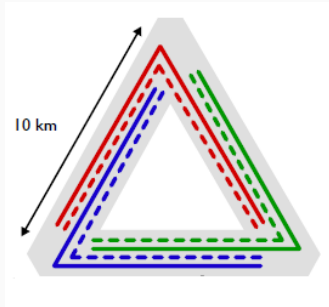


Figure 2: ET-D design

- Detect BH-BH mergers upto $z \sim 20$ @ 10^5 – 10^6 events/year
- Detect NS-NS mergers upto $z \sim 3$ @ 10^4 – 10^5 events/year
- * H_0 measurement to 1% uncertainty in 1 year of ET (You et al. 2021)
- 📍 Two candidate locations: *Island of Sardinia, Italy* OR *Meuse–Rhine Euroregion (near Belgium, Germany, Netherlands)*

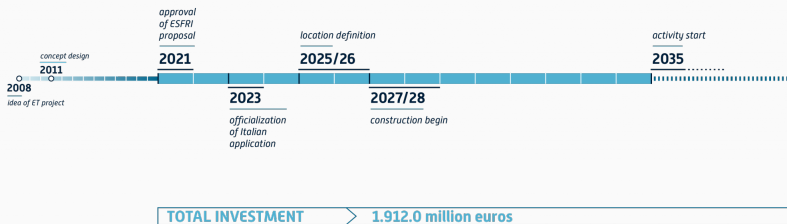


Figure 3: Timeline of ET

Image source: <https://www.einstein-telescope.it/en/einstein-telescope-en/>

Gravitational Wave Astronomy

- ◆ The strain (amplitude), h , in the interferometer arm of length, L , of a GW detector is given by

$$h(t) = \Delta L/L = \text{constant} \times \frac{\mathcal{M}^{5/3}}{d_L} f^{2/3} \Theta \cos \Phi$$

where $\mathcal{M} = \frac{(m_1 m_2)^{3/5}}{(m_1 + m_2)^{1/5}}$ is called the chirp mass of a binary.

- ◆ Due to the cosmological redshift of the incoming GW frequency, what we measure is the redshifted chirp mass, $\mathcal{M}_z = (1+z)\mathcal{M}$.
- ◆ Since a measured chirp mass can correspond to many chirp mass and redshift values, we get **mass-redshift degeneracy**.
- ◆ In the absence of an EM counterpart of the GW event, one can lift the degeneracy with the population method.

Cosmology

- ⊗ The current standard model of the universe is called the Λ -Cold Dark Matter (Λ CDM) model.
- ⊗ It is characterized by the parameters: $H_0, \Omega_m, \Omega_\Lambda, \Omega_{\text{rad}}, \Omega_k, w$
- ⊗ Hubble constant, H_0 , quantifies the expansion rate of the universe; lies around 70 km/s/Mpc.
- ⊗ By construction, $\Omega_m + \Omega_{\text{rad}} + \Omega_k + \Omega_\Lambda = 1$
- ⊗ In the minimal six-parameter model: $\Omega_{\text{rad}} \sim 0, \Omega_k = 0$ (flat), $w = -1$ so that $\Omega_\Lambda + \Omega_m = 1$

$$\text{Luminosity distance, } d_L = \frac{c}{H_0} (1+z) \int_0^z \frac{dz'}{\sqrt{\Omega_m(1+z')^3 + (1-\Omega_m)}}$$

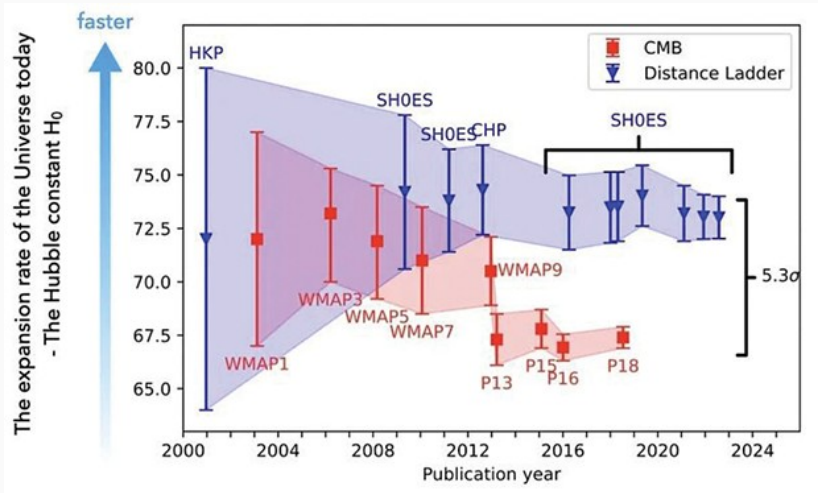


Figure 4: Plot showing conflicting H_0 measurements from two datasets (Image credit: William D'Arcy Kenworthy, Stockholm University)

- △ Measurements from Cepheids and Type Ia Supernovae (late universe) → **73.0 ± 1.0 km/s/Mpc** (SH0ES Collaboration; Riess et al. 2022)
- ▽ Measurements from Cosmic Microwave Background (CMB) (early universe) → **67.4 ± 0.5 km/s/Mpc** (Planck Collaboration; Aghanim et al. 2020)
- ◇ The divergence is found to be of $\sim 5\sigma$ significance.
- Measurements from Tip of the Red Giant Branch (TRGB) (late universe) → **69.8 ± 2.2 km/s/Mpc** (Freedman 2021)
- GW standard siren measurements can solve the discrepancy.

Method

- ☆ We generate a NS-NS binary merger population using the binary evolution code *StarTrack* (Belczynski et al. 2008, 2020).
- ☆ These NS binaries are analyzed using ET's design sensitivity.
- ☆ The ones which exceed the detection threshold ($\text{SNR}_{\text{eff}} > 8$ and at least one $\text{SNR}_i > 3$ for $i \in [1, 2, 3]$) are identified as events.
- ☆ Using a cosmological model, the luminosity distance for each detected event is measured from the observable quantities.

Given data: $P(\mathcal{M})$, $P(\mathcal{M}_z)$, $P(d_L)$, $\Omega_m = 0.3$, $\Omega_\Lambda = 1 - \Omega_m = 0.7$, $w = -1$

$$\because \mathcal{M}_z = \mathcal{M}(1+z) \implies z = \frac{\mathcal{M}_z}{\mathcal{M}} - 1$$

Probability distribution of z :

$$P(z) = \int d\mathcal{M}_z P(\mathcal{M}_z) \int d\mathcal{M} P(\mathcal{M}) \delta\left(z - \left(\frac{\mathcal{M}_z}{\mathcal{M}} - 1\right)\right)$$

$$\because H_0 \equiv H_0(z, d_L) = \frac{c}{d_L} (1+z) \int_0^z \frac{dz'}{\sqrt{\Omega_m (1+z')^3 + (1-\Omega_m)}}$$

Probability distribution of H_0 :

$$P(H_0) = \int dz P(z) \int dd_L P(d_L) \delta(H_0 - H_0(z, d_L))$$

We find the cumulative probability from the probability density as:

$$CP(H_0) = \int_0^{H_0} P(H'_0) dH'_0$$



This function ranges from 0 to 1 and equals 0.5 at the median of the probability distribution.



For 90% confidence interval, we get the lower and upper bounds when $CP = 0.05$ and $CP = 0.95$ respectively.



Next, we calculate the function, $CP \times (1 - CP)$, which ranges from 0 to 0.25 and peaks at the median of the probability distribution.



We repeat the above steps for every event. Finally, we compute the product, $\prod CP \times (1 - CP)$, and scale it so that the peak is 0.25.

Results

We simulated 50000 NS-NS mergers of which 5940 were marked as detected. Measurables for those events constitute the mock data.

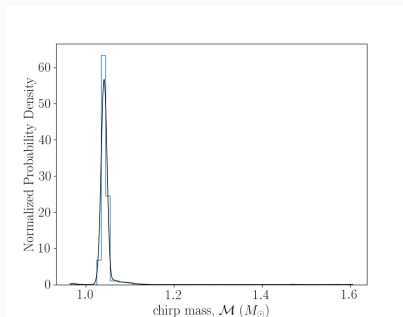


Figure 5: $P(\mathcal{M})$ used in the study based on the binary evolution model M30.B. Here, $\mathcal{M}_{\min} = 0.96 M_{\odot}$ and $\mathcal{M}_{\max} = 1.60 M_{\odot}$. The distribution is represented by the blue histogram with binsize $0.01 M_{\odot}$.

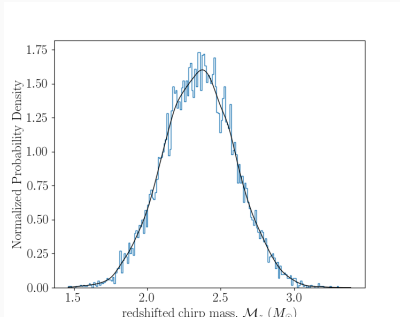


Figure 6: $P(\mathcal{M}_z)$ for one of the events. The distribution is represented by the blue histogram with binsize $0.01 M_{\odot}$. This $P(\mathcal{M}_z)$ is to be used as input together with $P(\mathcal{M})$ to determine $P(z)$ for this specific event.

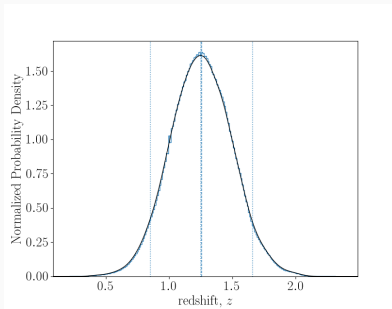


Figure 7: $P(z)$ for the same event. Middle dotted line shows the median of the distribution. The left and right dotted lines show the 90% confidence interval. Dashed line shows the injected value. The distribution is shown by the blue histogram with binsize 0.01.

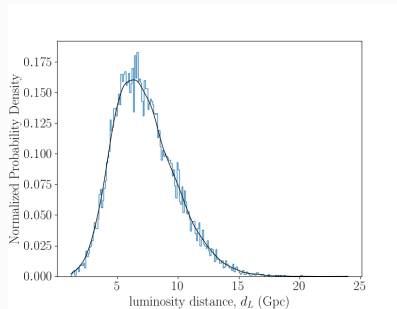


Figure 8: $P(d_L)$ for the same event. The distribution is shown by the blue histogram with binsize 0.1 Gpc. This $P(d_L)$ is to be used as input together with $P(z)$ to determine $P(H_0)$ for this specific event.

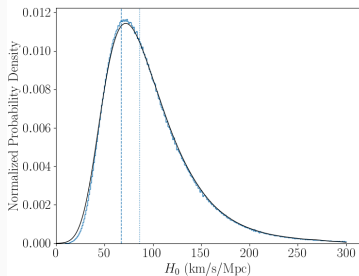


Figure 9: $P(H_0)$ for the same event. Dotted line shows the median of the distribution. Dashed line shows the injected value. The distribution is represented by the blue histogram with binsize 1 km/s/Mpc. The smooth curve denotes the distribution with binsize 0.1 km/s/Mpc.

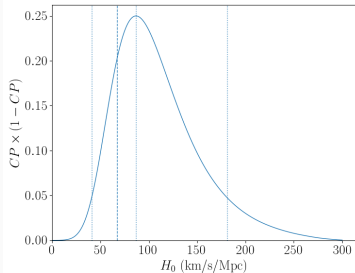


Figure 10: $CP \times (1 - CP)$ for H_0 (normalized) with stepsize 0.1 km/s/Mpc. Middle dotted line shows the median of the distribution. Left and right dotted lines mark the 90% confidence interval. Dashed line shows the injected value of 67.3 km/s/Mpc.

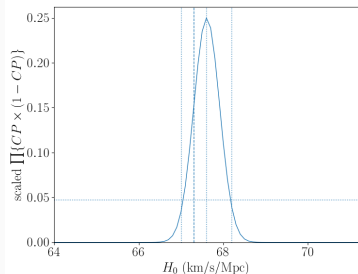


Figure 11: Combined $CP \times (1 - CP)$ for H_0 with stepsize 0.1 km/s/Mpc. Middle dotted line shows the median of the H_0 distribution. Left and right dotted lines mark the 90% confidence interval. Dashed line shows the injected value of 67.3 km/s/Mpc. The estimate obtained is $H_0 = 67.6 \pm 0.6$ km/s/Mpc.

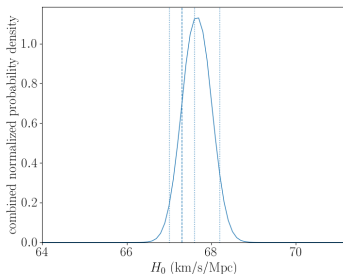
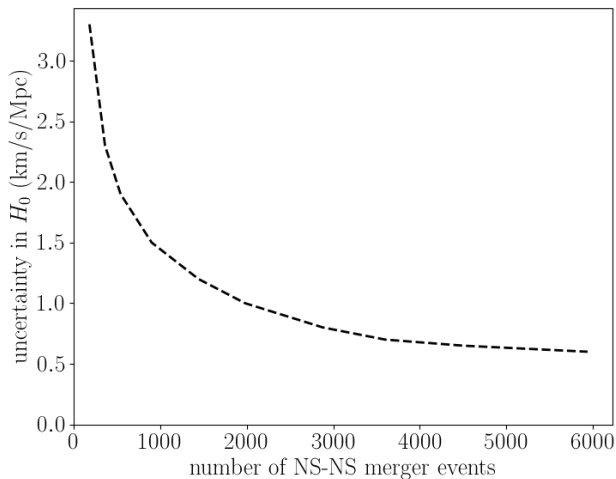






Figure 12: Combined $P(H_0)$ (normalized) with stepsize 0.1 km/s/Mpc. Middle dotted line shows the median of the distribution. Left and right dotted lines mark the 90% confidence interval. Dashed line shows the injected value of 67.3 km/s/Mpc. The estimate obtained is $H_0 = 67.6 \pm 0.6$ km/s/Mpc.

The uncertainty in H_0 drops inversely as $\sim 1/\sqrt{N}$ with number of events, and becomes less than 1% for more than ~ 5000 events.



-  If the true chirp mass lies at the extremes of the intrinsic chirp mass distribution, the mass-redshift degeneracy is not lifted.
-  In that case, as $P(\mathcal{M}) \approx 0$ so that $P(z) \approx 0$ at the actual z , and we get an entirely wrong redshift, and thus, a bad H_0 estimate.
-  We encountered ~ 15 such instances out of the total 5940 events. But we did not eliminate any. Negligible effect on final result.
-  NS-NS events are very few and restricted to low redshifts. Hence, evolution of H_0 with z is hard to ascertain through them.

Conclusion

- ▶ We demonstrated a method of determining H_0 using only GW data from Einstein Telescope.
- ▶ We found that uncertainty will fall below 1% if more than 5000 NS-NS events are detected with ET (i.e. 1 month of observation).
- ▶ We will analyze ET mock data generated for various other binary evolution models.
- ▶ We will do similar analyses for BH-BH events and compare the result with that obtained from NS-NS events.
- ▶ We will estimate other cosmological parameters and quantify the accuracy that can be achieved.



Belczynski et al.

Evolutionary roads leading to low effective spins, high black hole masses, and O1/O2 rates for LIGO/Virgo binary black holes

Astronomy & Astrophysics, 2020



Singh & Bulik

Constraining parameters of coalescing stellar mass binary black hole systems with the Einstein Telescope alone

Physical Review D, 2021

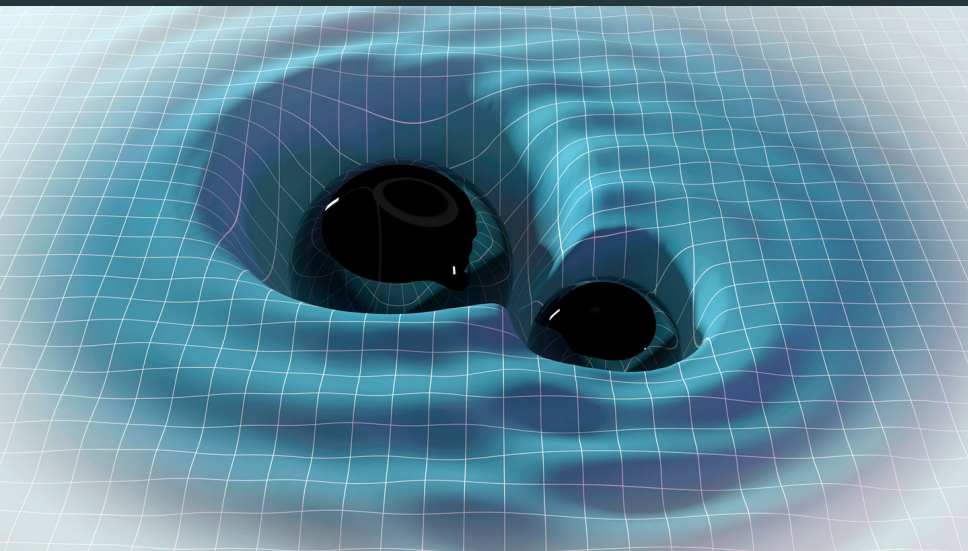


Singh & Bulik

Constraining parameters of low mass merging compact binary systems with Einstein Telescope alone

Physical Review D, 2022

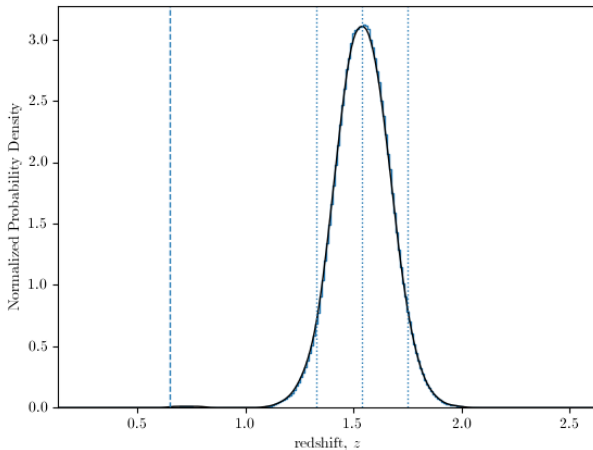
That's all!



QUESTIONS ?

Results - exception

The injected redshift value is 0.65 and recovered value is 1.55 because of an extreme chirp mass value of $1.6 M_{\odot}$.



Gravitational Waves

- ☞ GW are spacetime deformations that move at the speed of light.
- ☉ Astrophysical sources: compact binaries, rotating neutron stars, short duration bursts and stochastic GW background.
- ☉ GW distort the plane transverse to the propagation axis in two ways: h_+ and h_\times polarizations.
- ☉ This property is used to detect them using km-scale Michelson interferometers and high-power lasers.

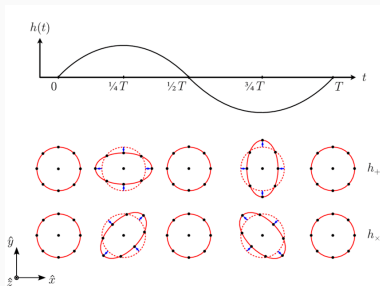


Figure 13: GW polarizations
(Le Tiec & Novak 2016)

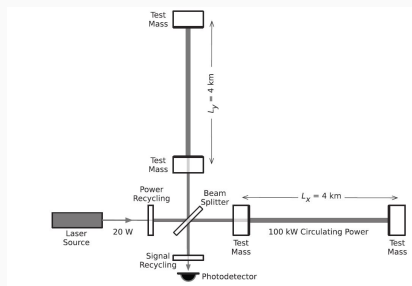


Figure 14: Laser Interferometer
(Abott et al. 2016)